Supporting Information

Synthesis of D-glucono-1,4-lactones modified with linear saturated fatty acids, novel low molecular-weight organogelators, and evaluation of their physical properties

Shiro Komba*

Institute of Food Research, National Agriculture and Food Research Organization, 2-1-12 Kannondai, Tsukuba, Ibaraki 305-8642, Japan

*Correspondence: skomba@affrc.go.jp; Tel.: +81-29-838-7298

TABLE OF CONTENTS

1. NMR charts

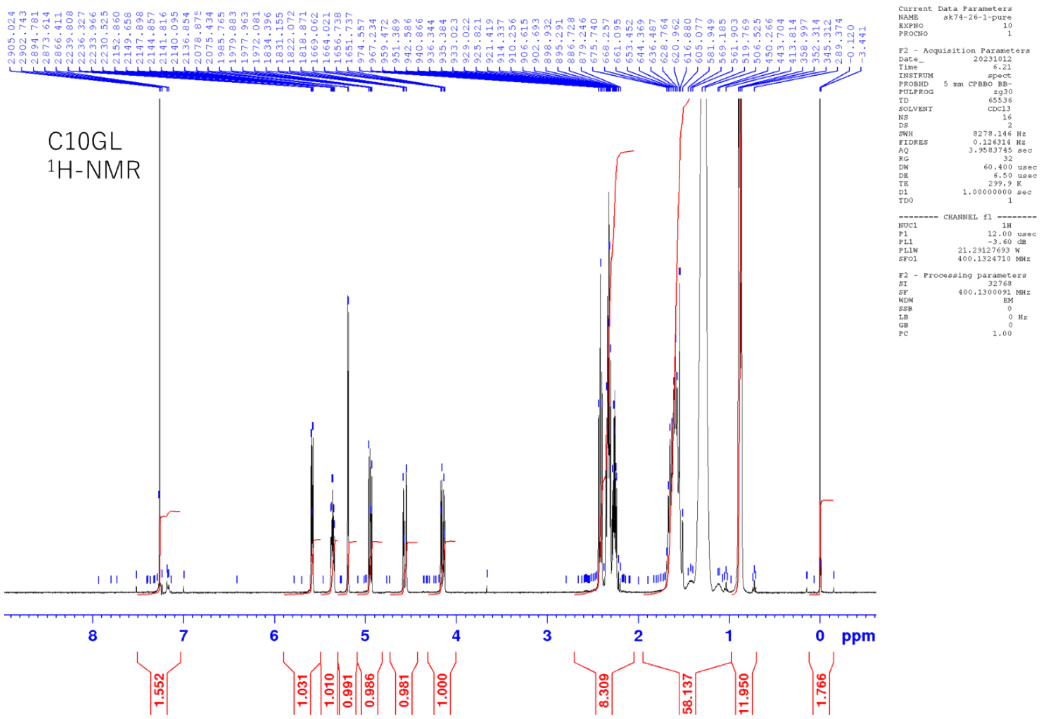

Figure S1. ^{1}H-NMR chart of C10GL (**1**).

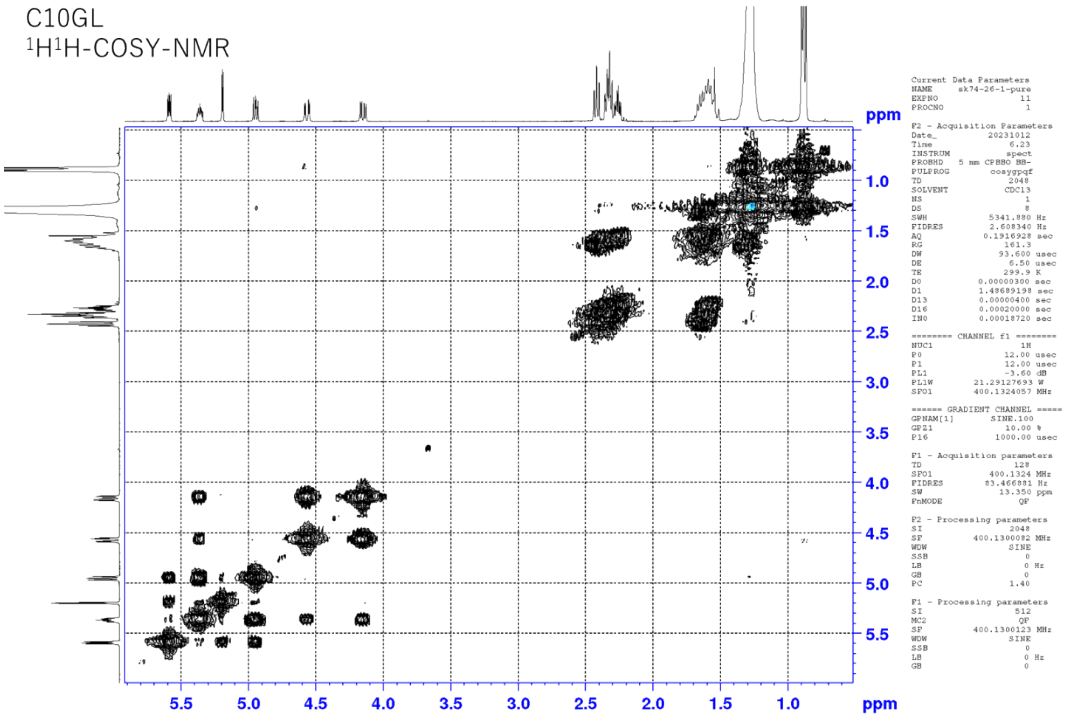

Figure S2. ^{1}H^{1}H -COSY-NMR chart of C10GL (**1**).

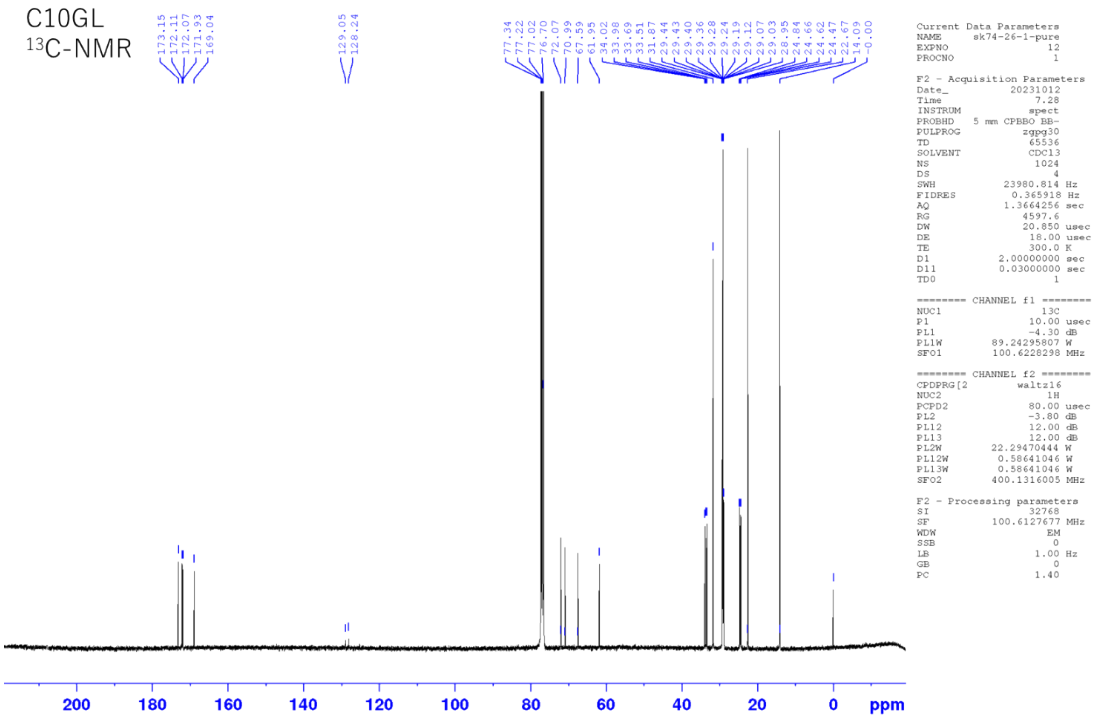

Figure S3. ^{13}C-NMR chart of C10GL (**1**).

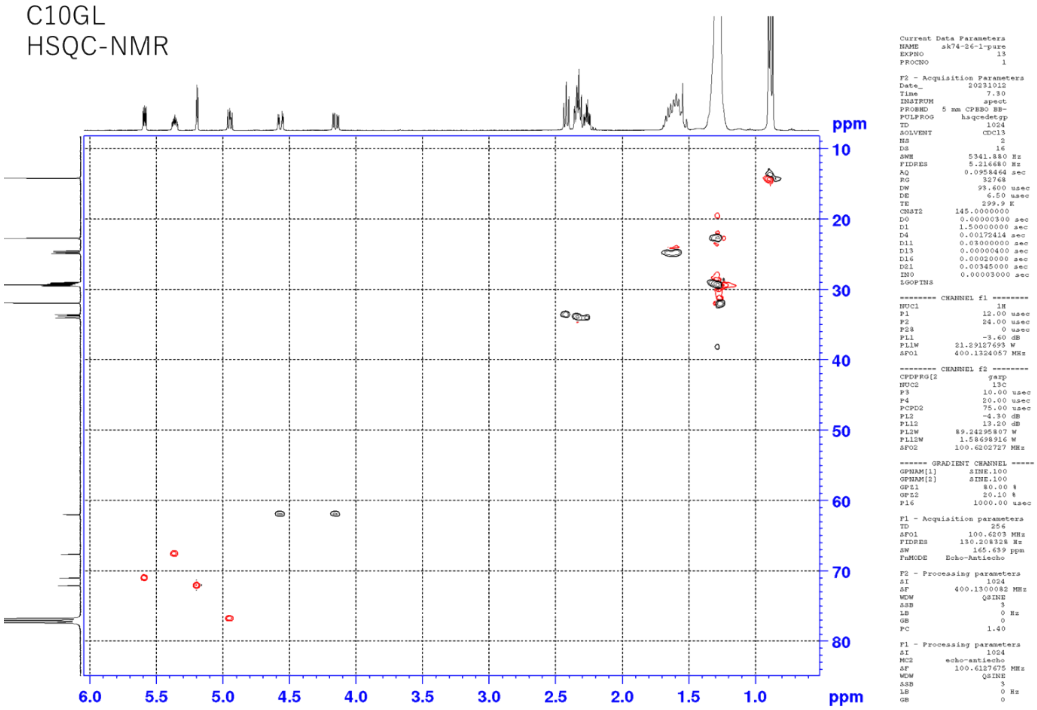

Figure S4. HSQC-NMR chart of C10GL (**1**).

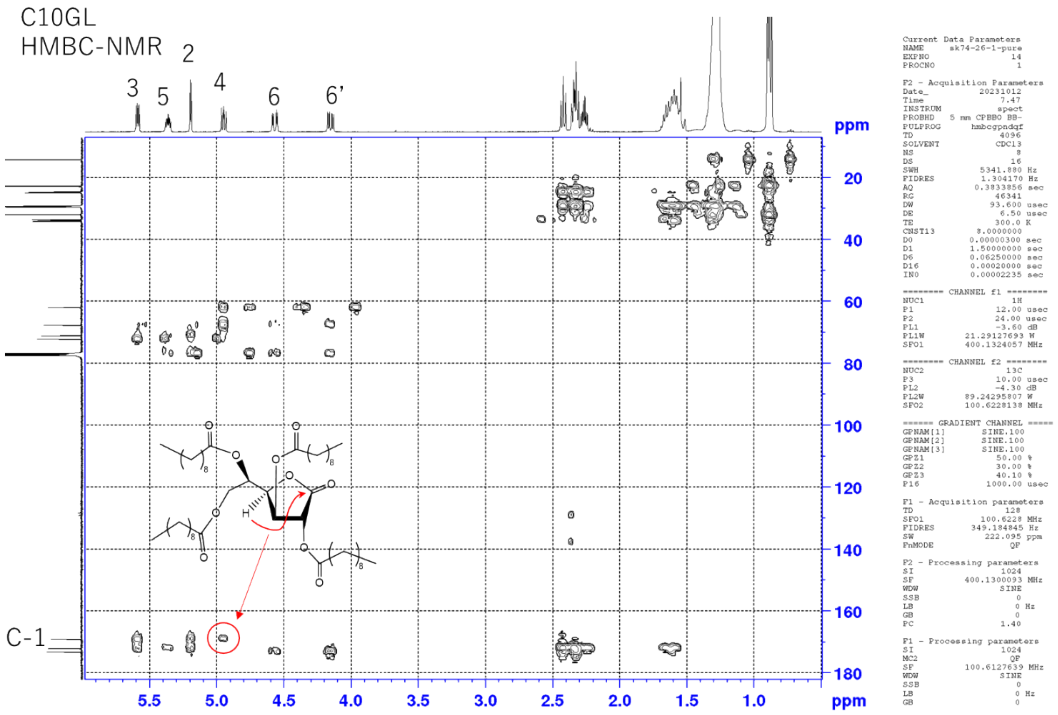

Figure S5. HMBC-NMR chart of C10GL (**1**).

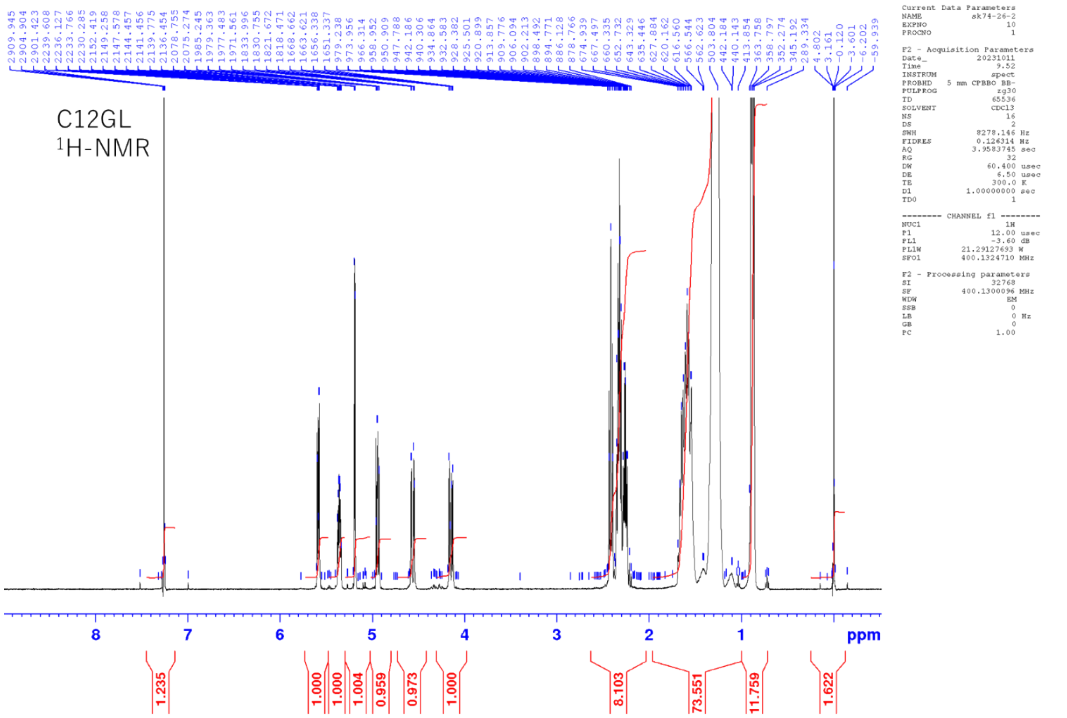

Figure S6. ^{1}H-NMR chart of C12GL (**2**).

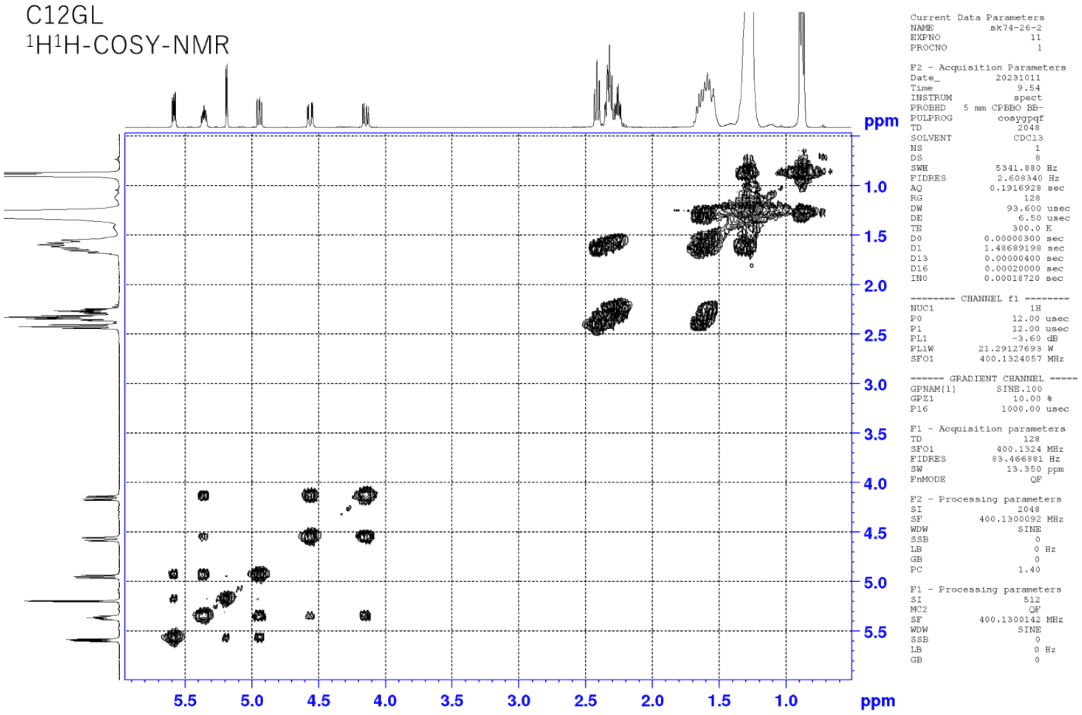

Figure S7. ^{1}H^{1}H-COSY-NMR chart of C12GL (**2**).

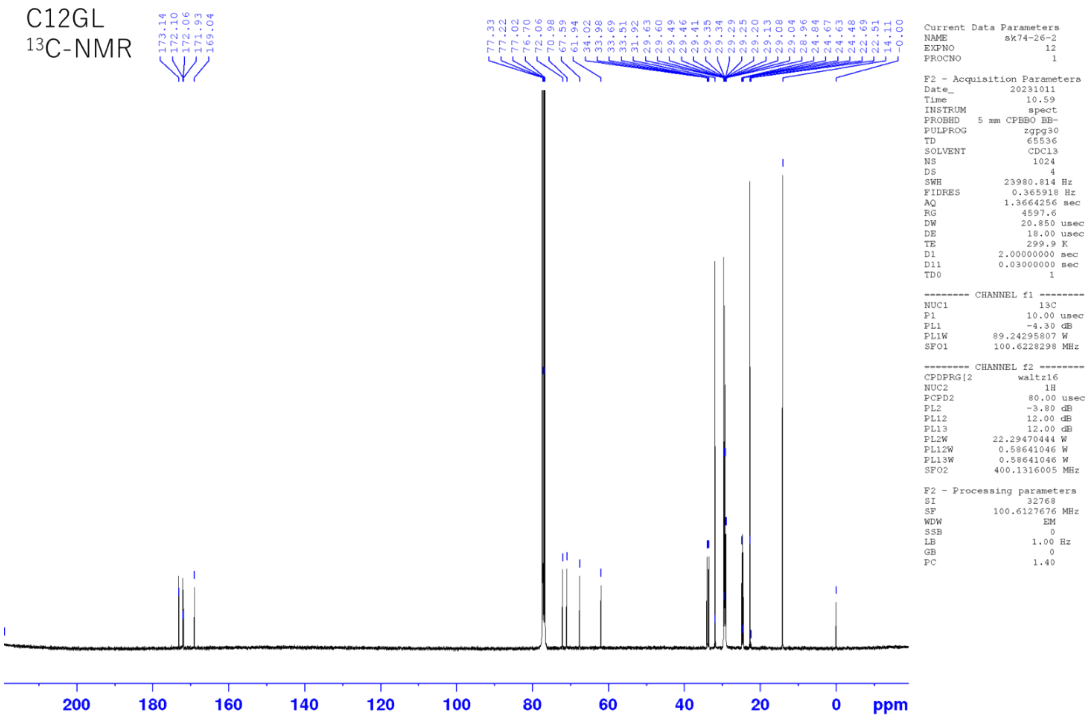

Figure S8. ^{13}C-NMR chart of C12GL (**2**).

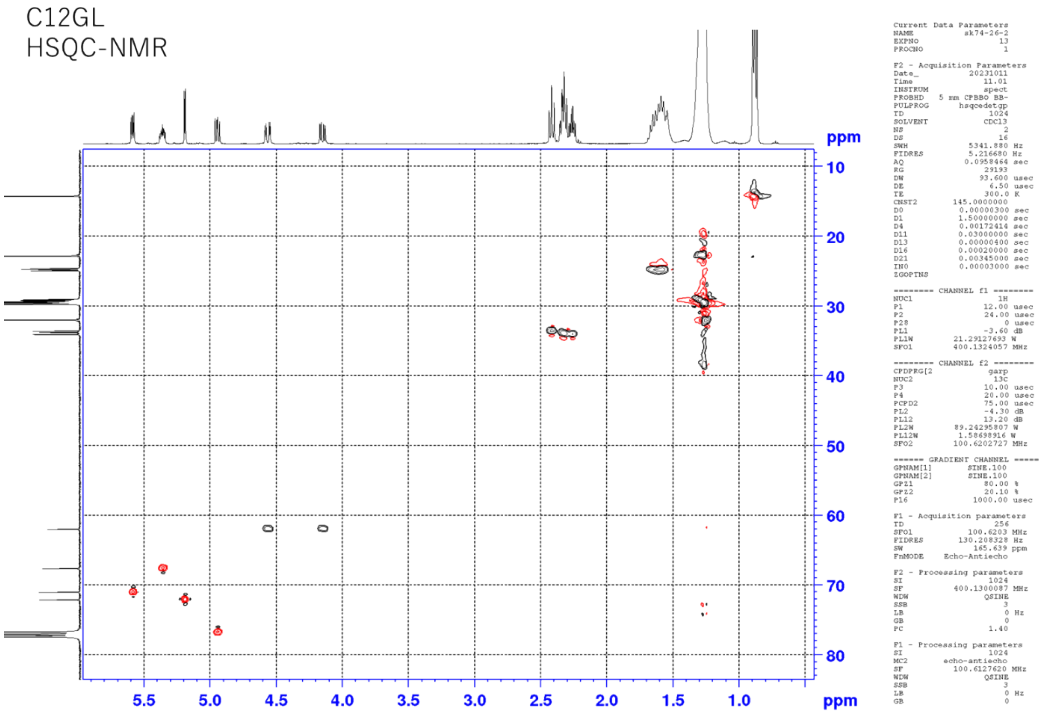

Figure S9. HSQC-NMR chart of C12GL (**2**).

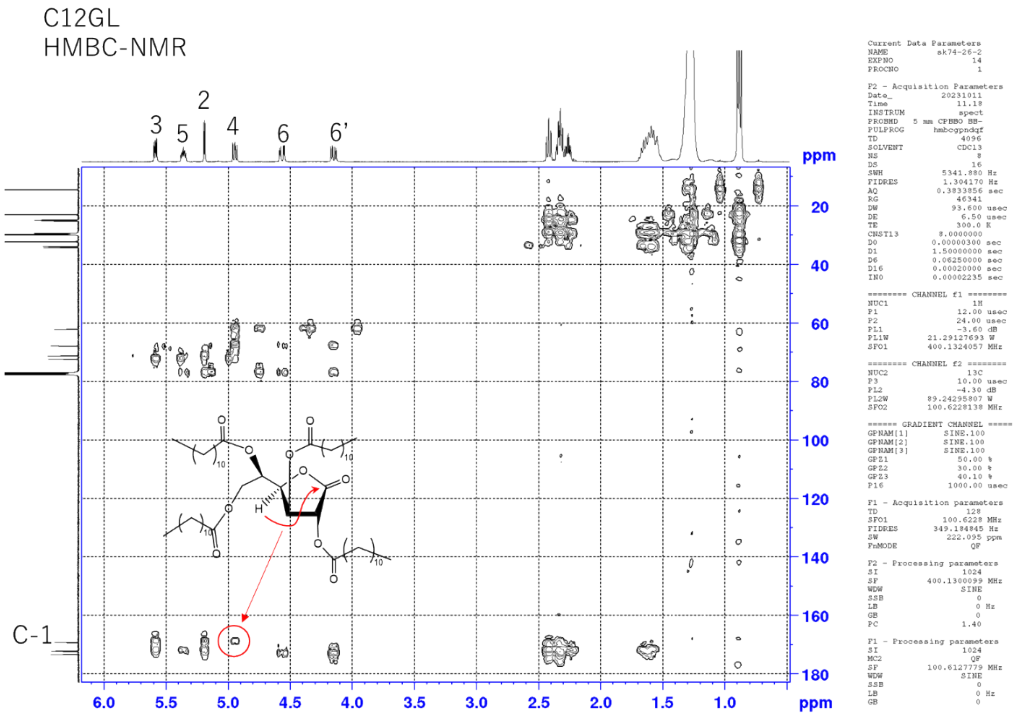

Figure S10. HMBC-NMR chart of C12GL (**2**).

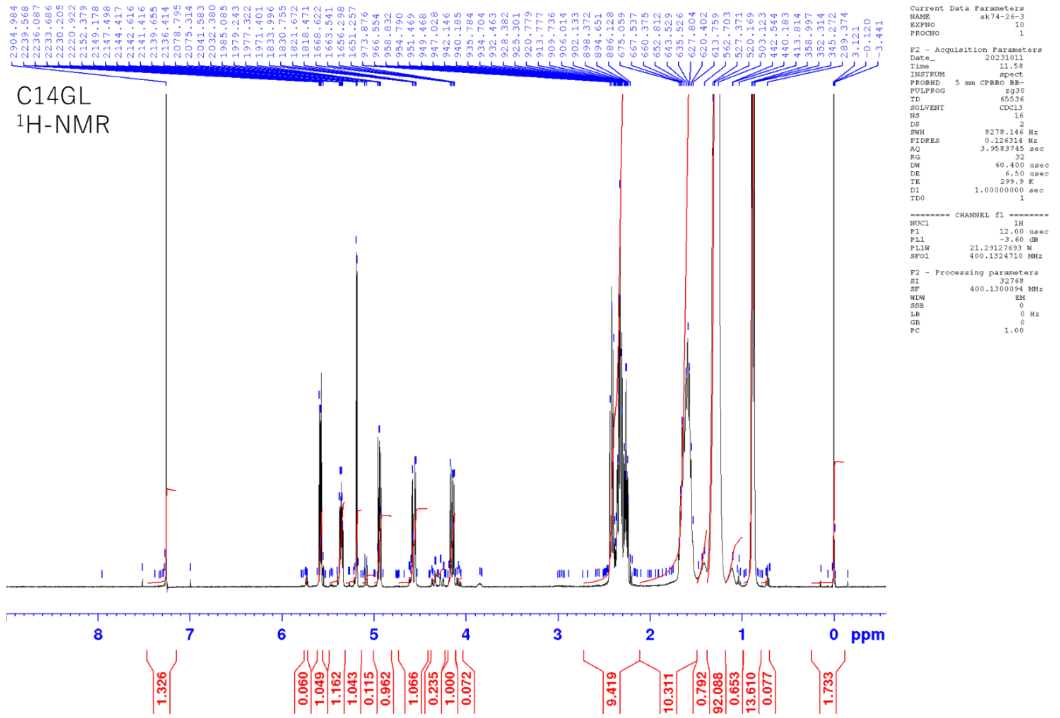

Figure S11. ^{1}H-NMR chart of C14GL (**3**).

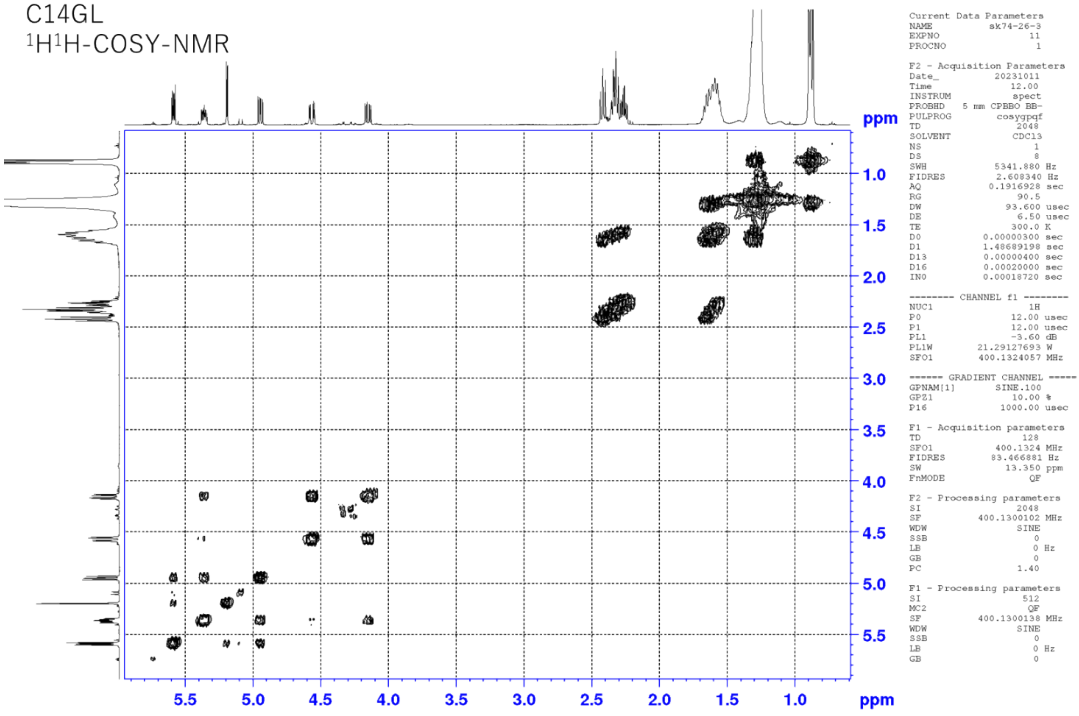

Figure S12. ^{1}H^{1}H-COSY-NMR chart of C14GL (**3**).

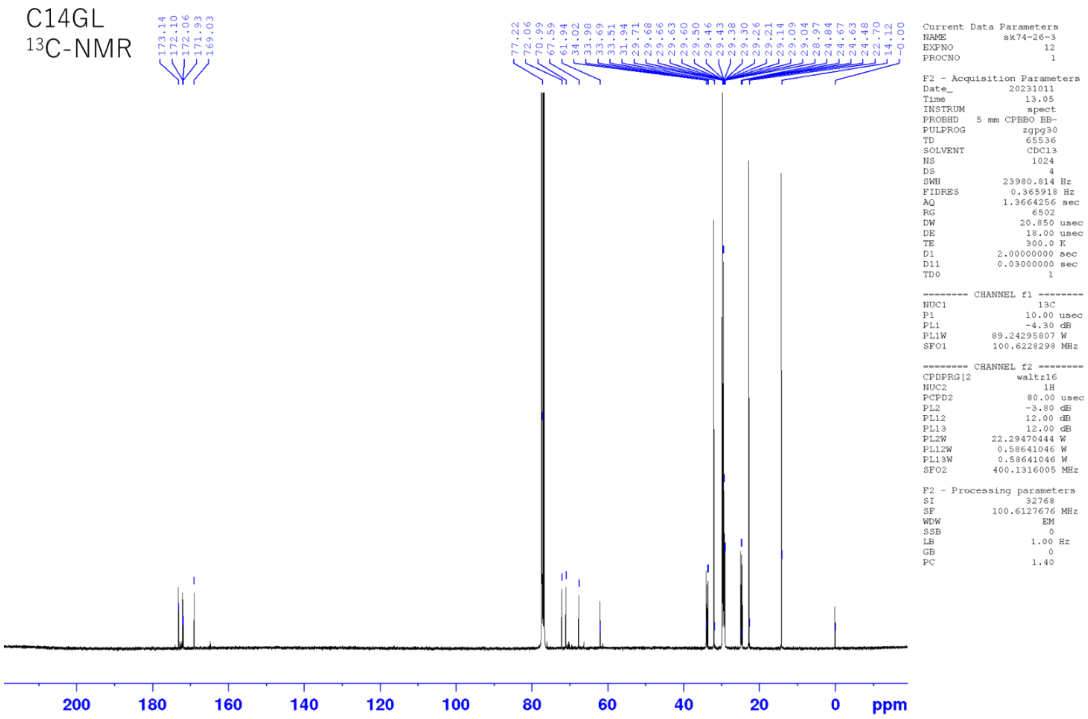

Figure S13. ^{13}C-NMR chart of C14GL (**3**).

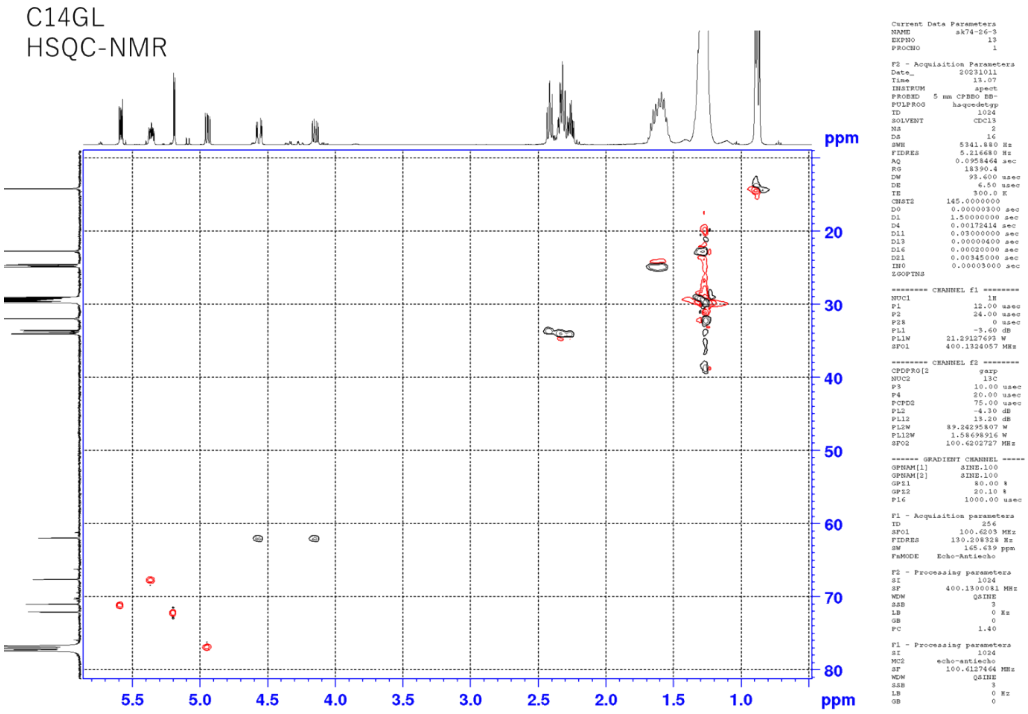

Figure S14. HSQC-NMR chart of C14GL (**3**).

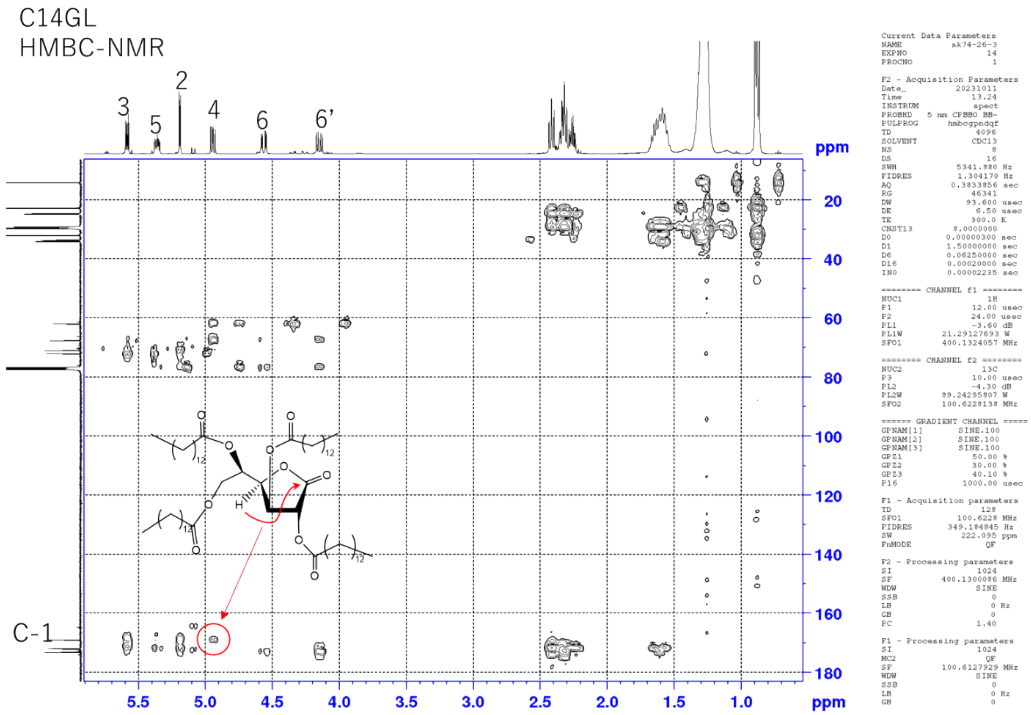

Figure S15. HMBC-NMR chart of C14GL (**3**).

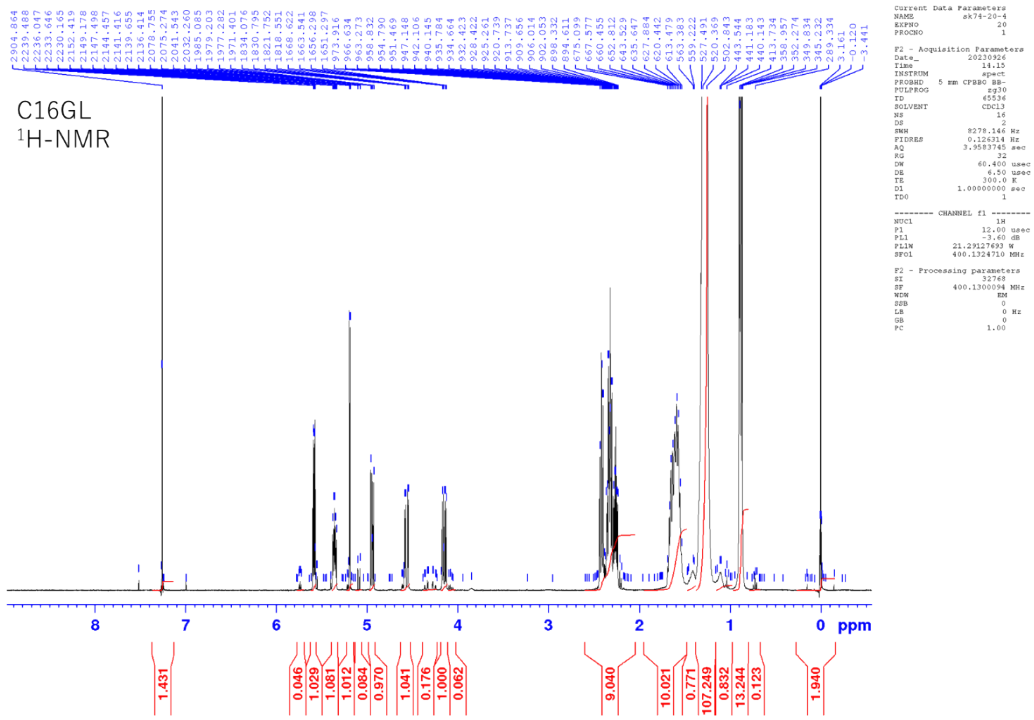

Figure S16. ^{1}H-NMR chart of C16GL (**4**).

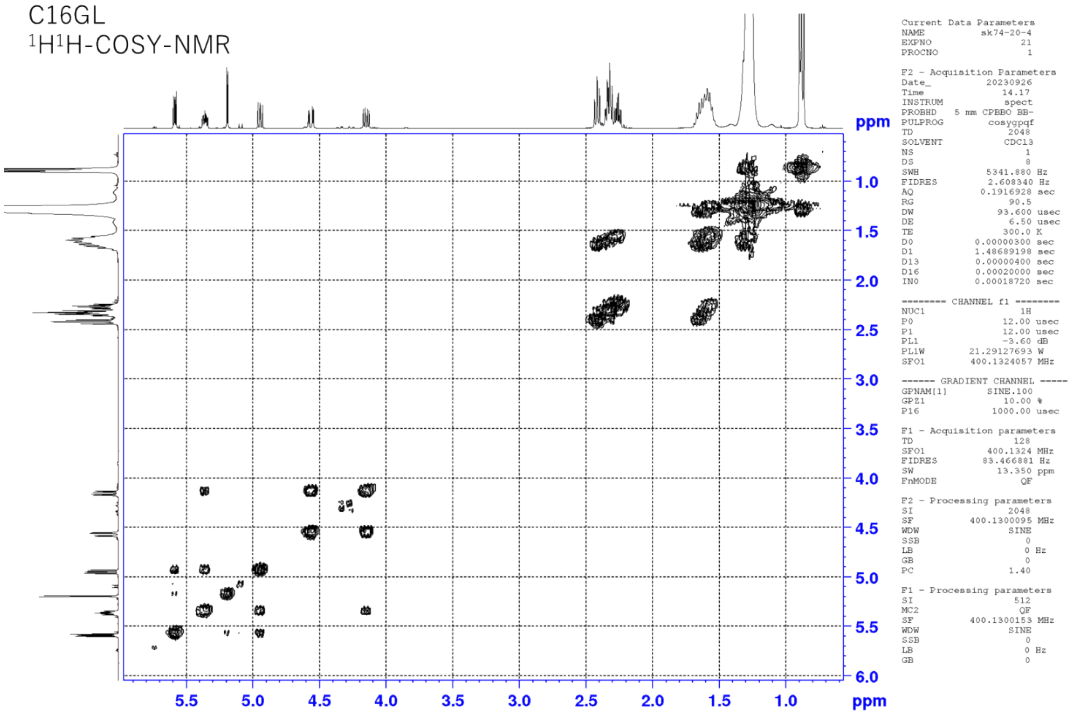

Figure S17. ^{1}H^{1}H-COSY-NMR chart of C16GL (**4**).

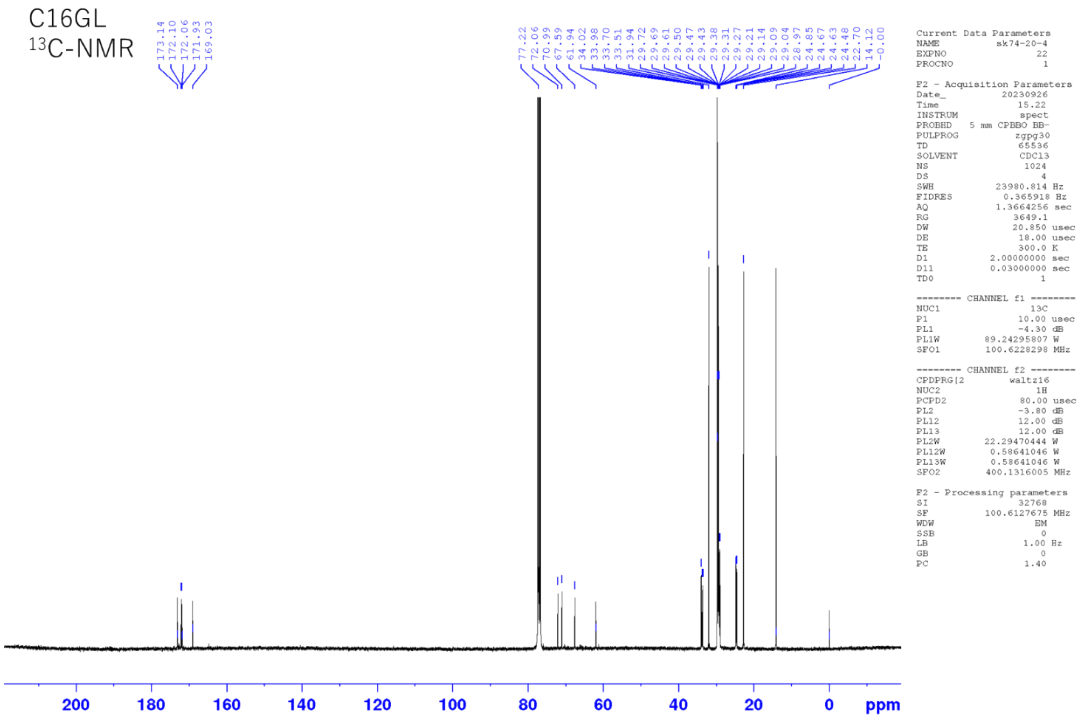

Figure S18. ^{13}C-NMR chart of C16GL (**4**).

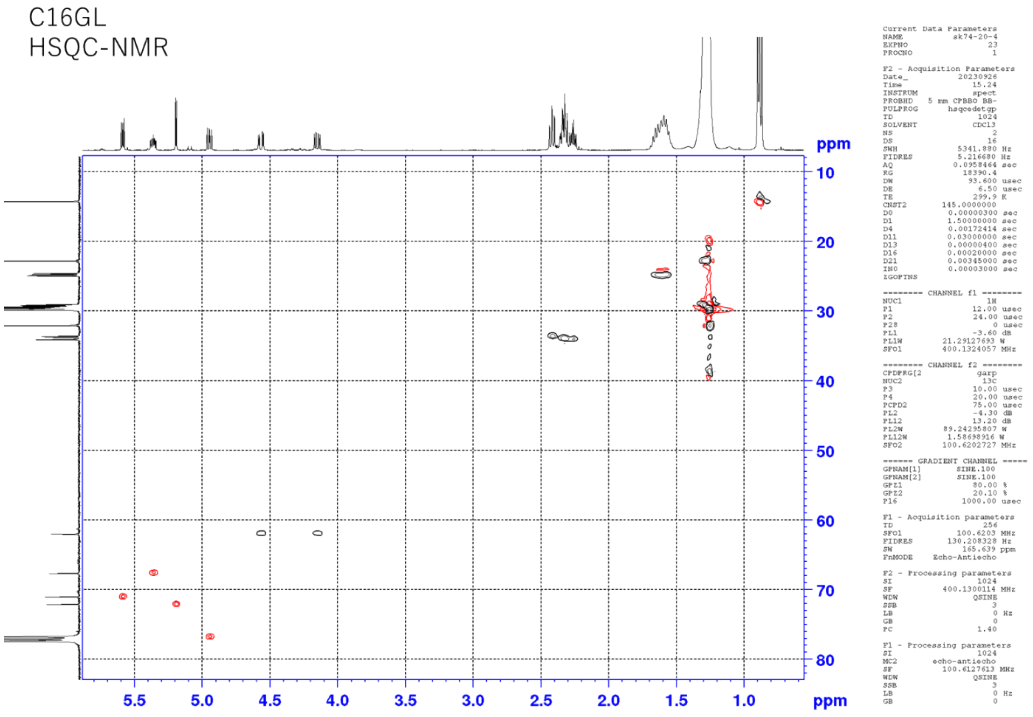

Figure S19. HSQC-NMR chart of C16GL (**4**).

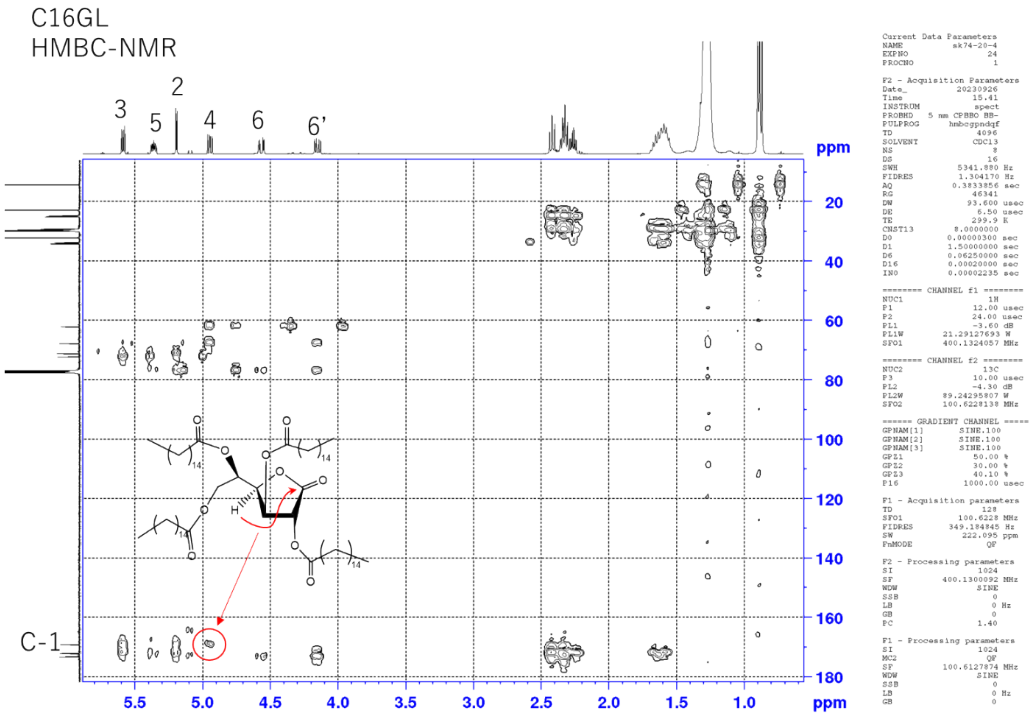

Figure S20. HMBC-NMR chart of C16GL (**4**).

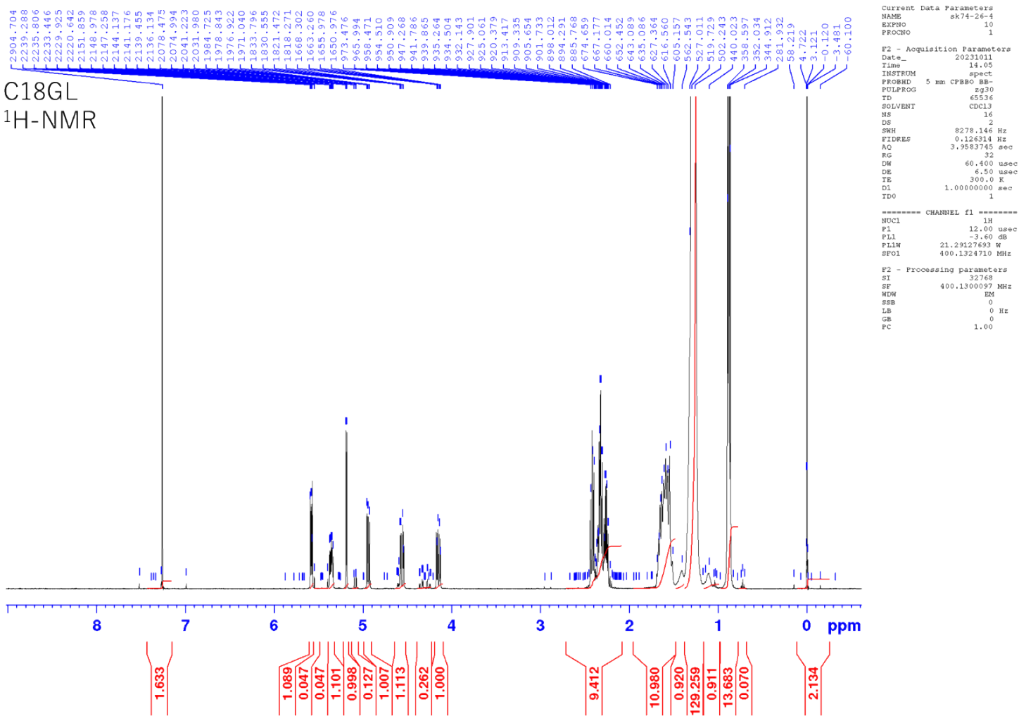

Figure S21. ^{1}H-NMR chart of C18GL (**5**).

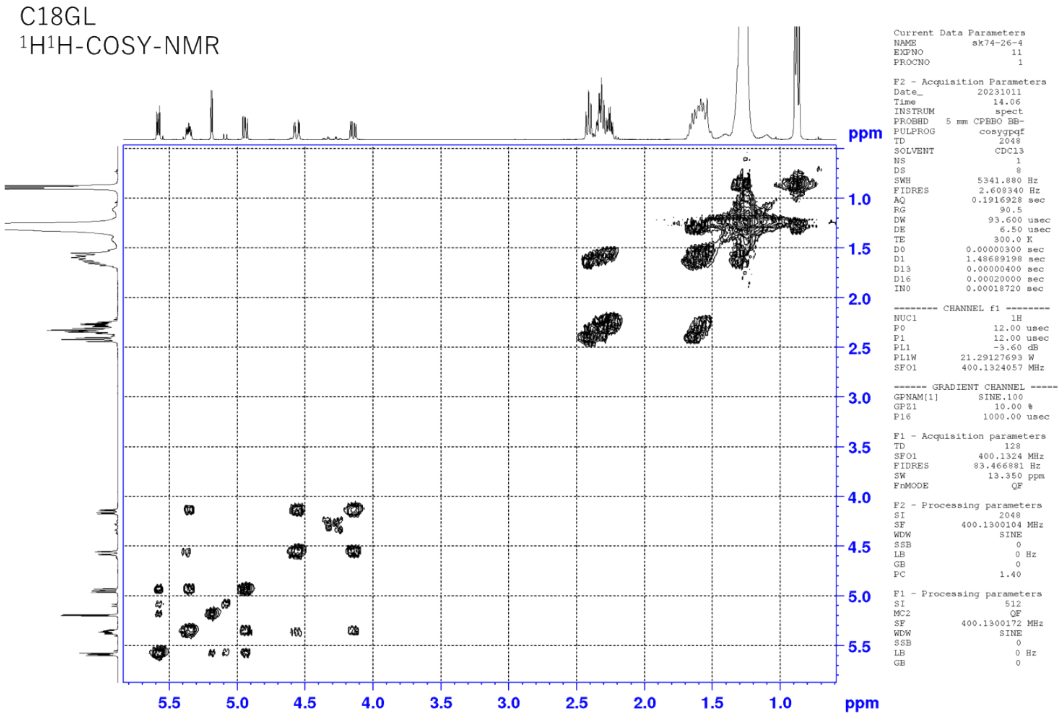

Figure S22. ^{1}H^{1}H-COSY-NMR chart of C18GL (**5**).

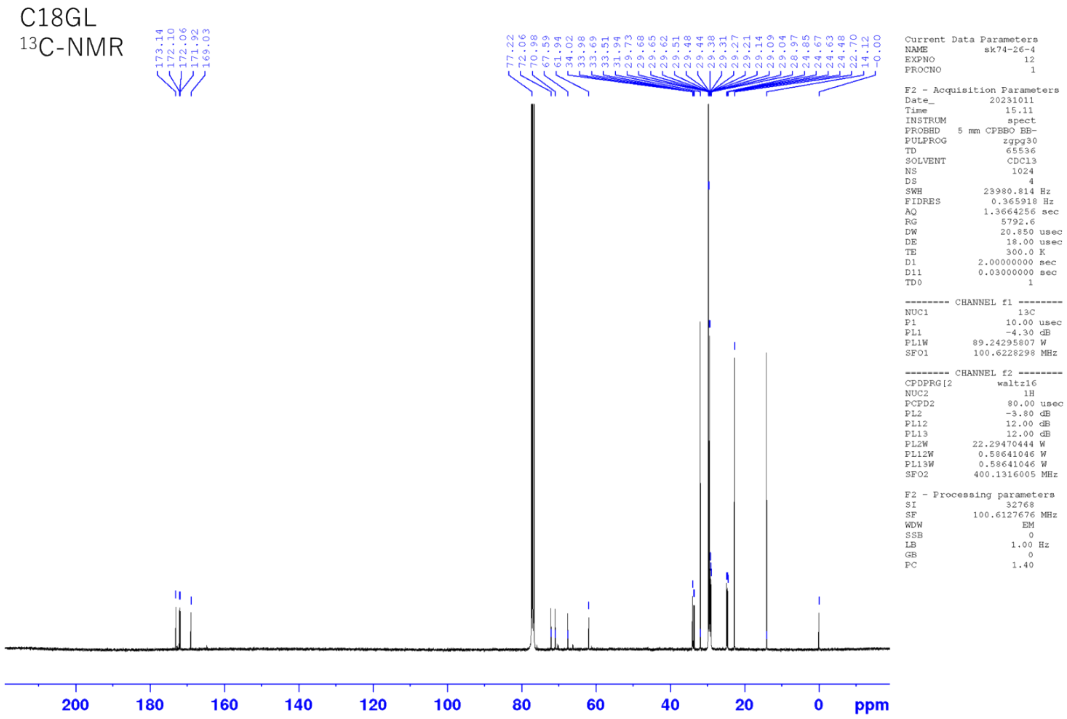

Figure S23. ^{13}C-NMR chart of C18GL (**5**).

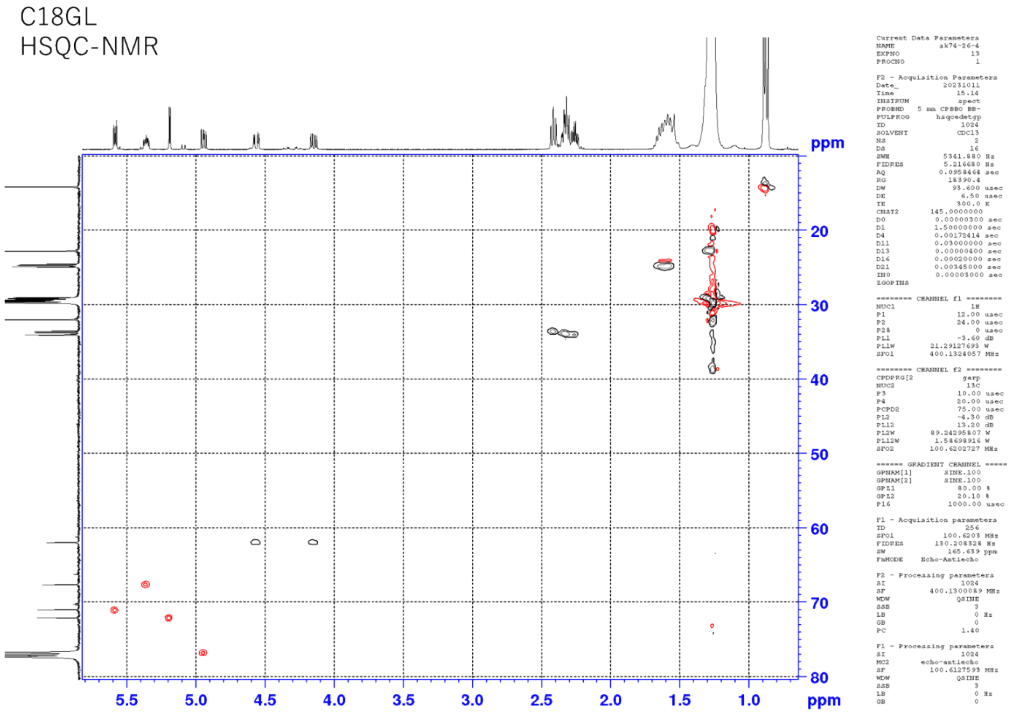

Figure S24. HSQC-NMR chart of C18GL (**5**).

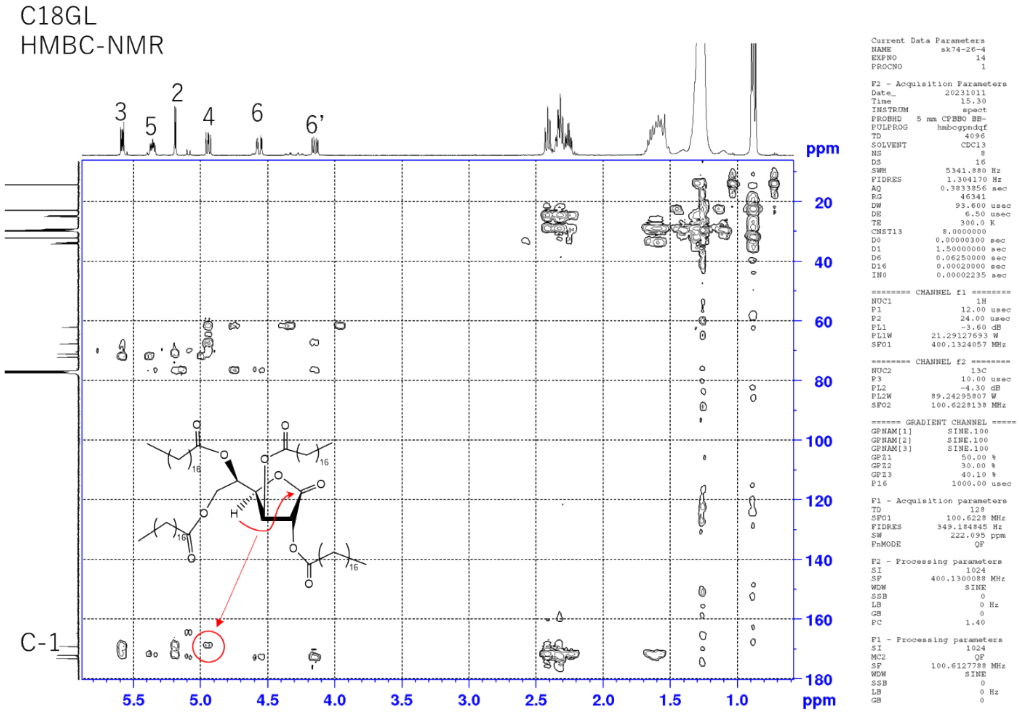

Figure S25. HMBC-NMR chart of C18GL (**5**).

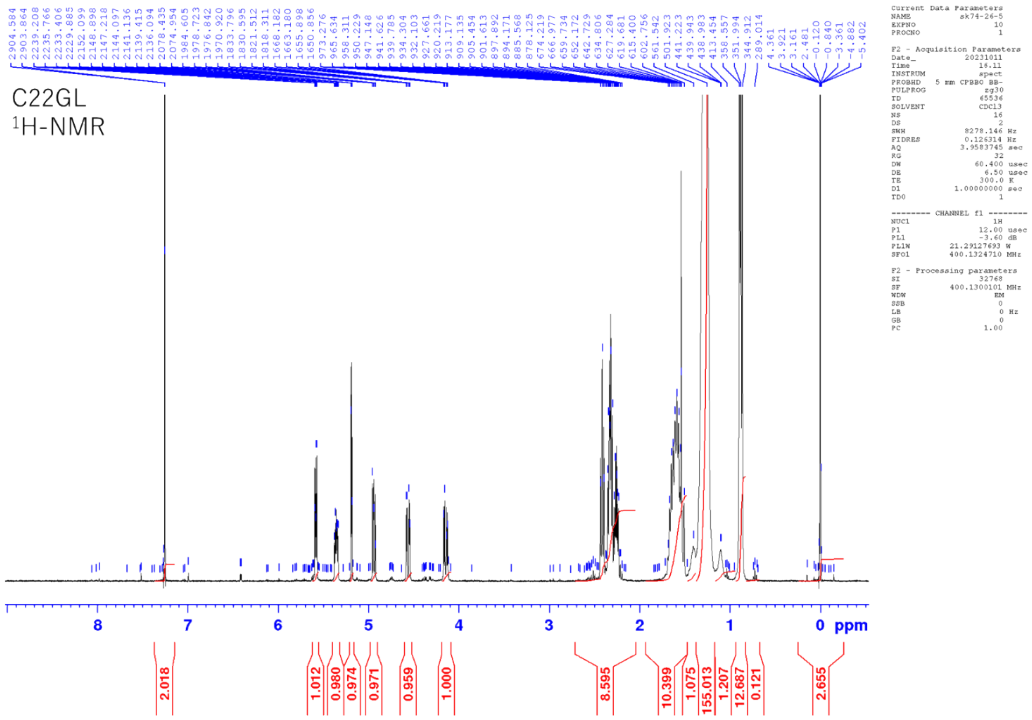

Figure S26. ^{1}H-NMR chart of C22GL (**6**).

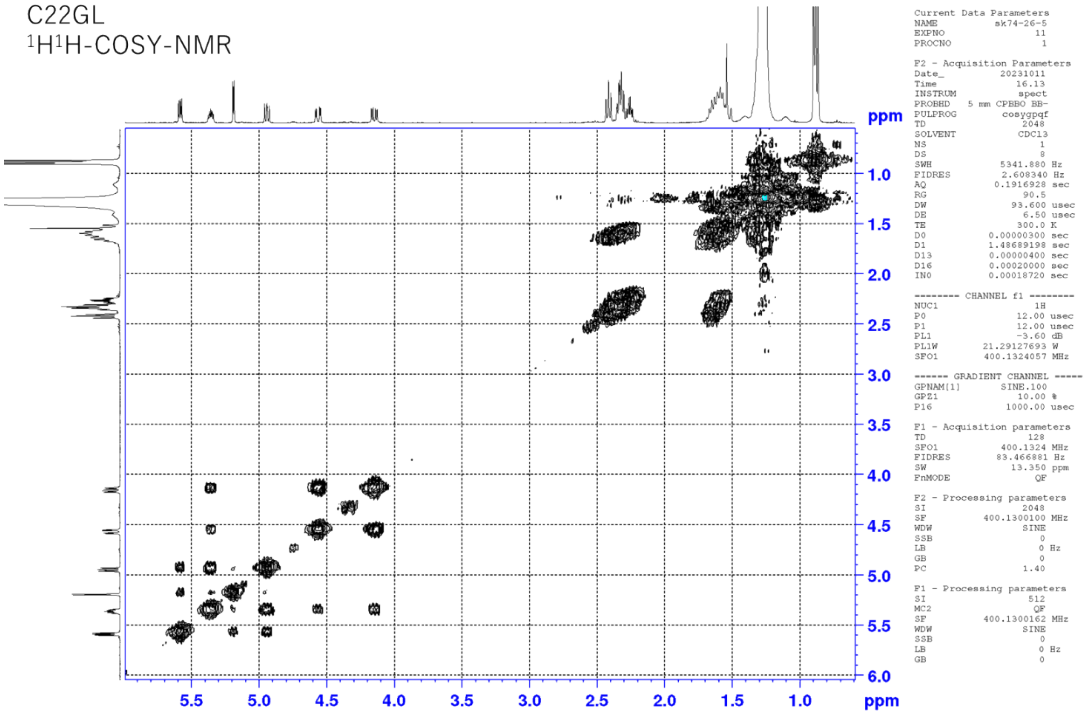

Figure S27. ^{1}H^{1}H-COSY-NMR chart of C22GL (**6**).

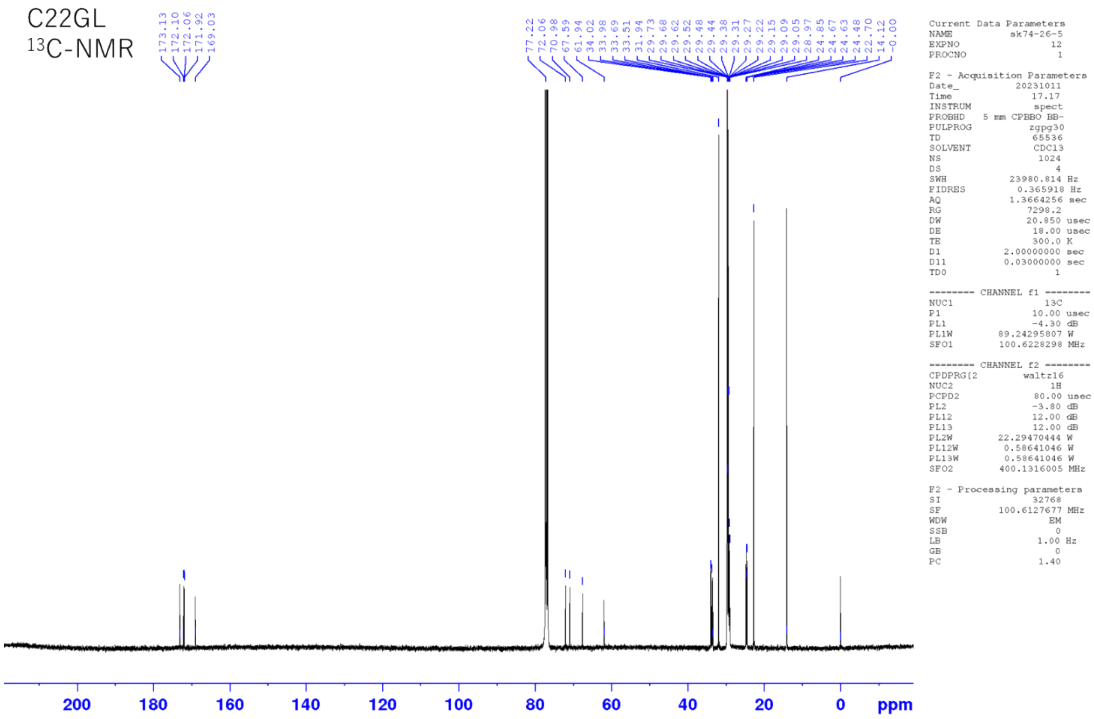

Figure S28. ^{13}C-NMR chart of C22GL (**6**).

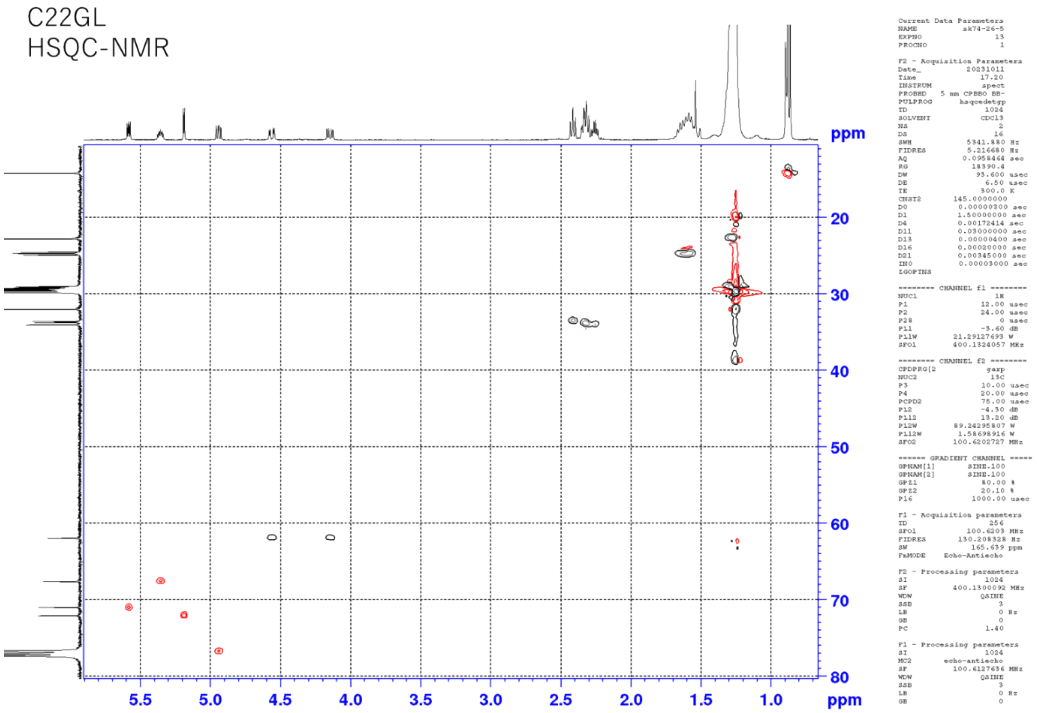

Figure S29. HSQC-NMR chart of C22GL (**6**).

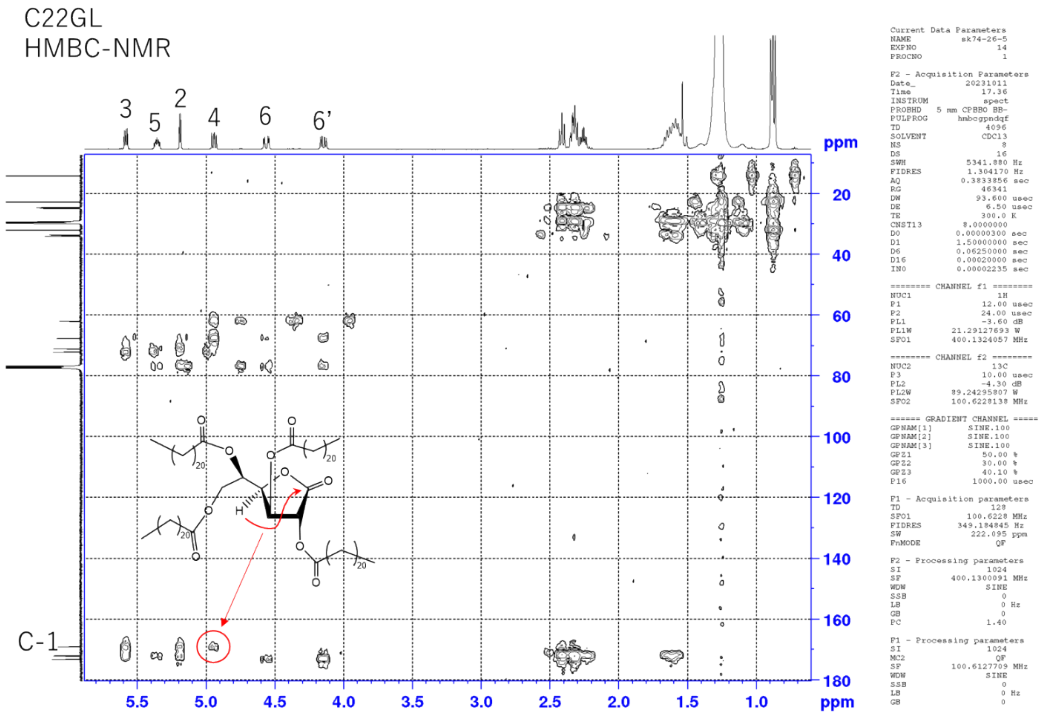

Figure S30. HMBC-NMR chart of C22GL (**6**).

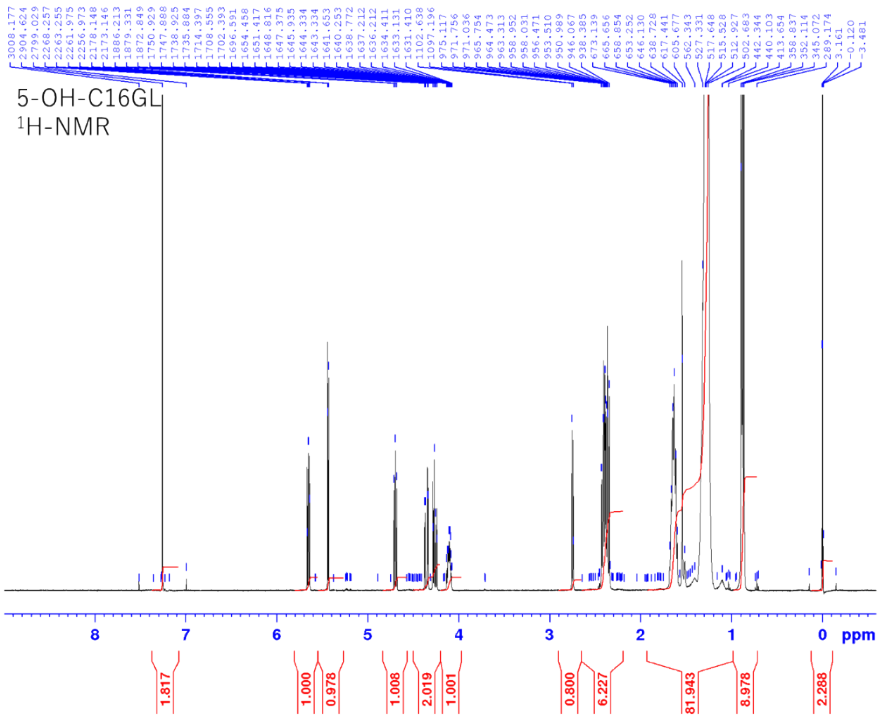

Figure S31. ^{1}H-NMR chart of 5-OH-C16GL (**7**).

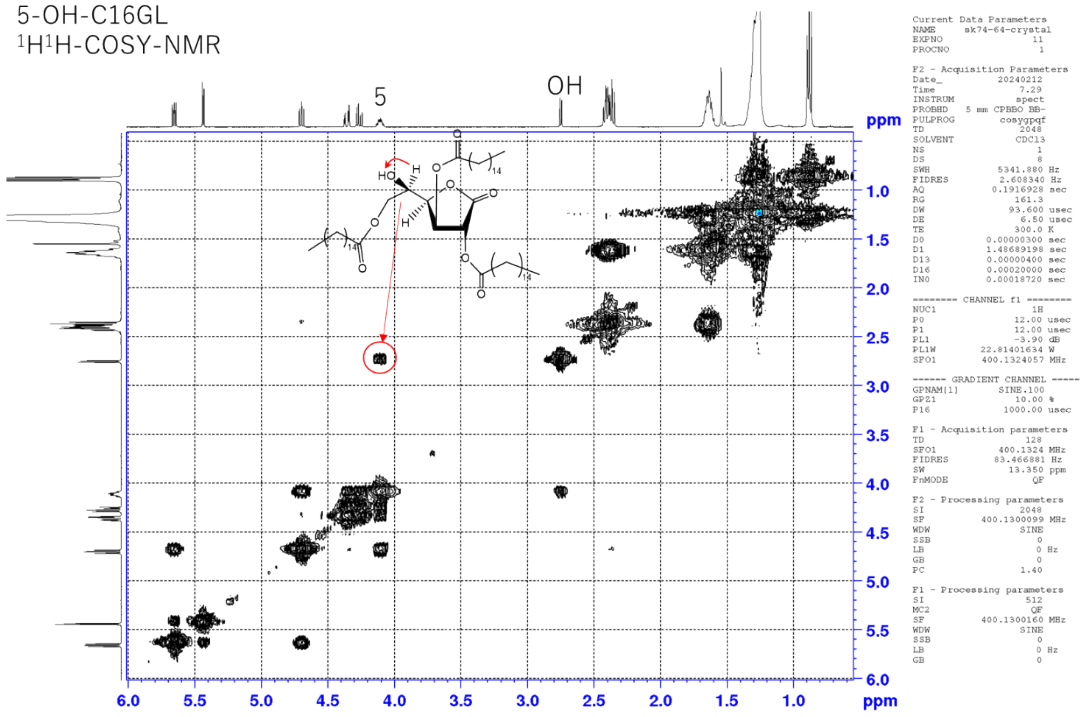

Figure S32. ^{1}H^{1}H-COSY-NMR chart of 5-OH-C16GL (**7**).

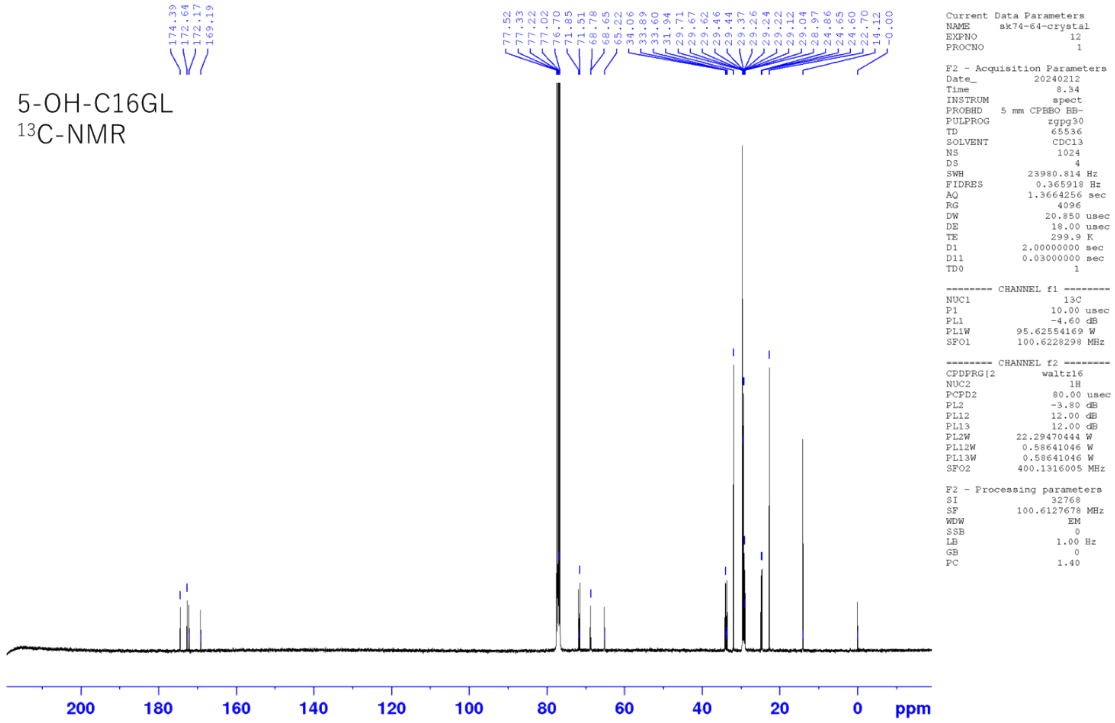

Figure S33. ^{13}C-NMR chart of 5-OH-C16GL (**7**).

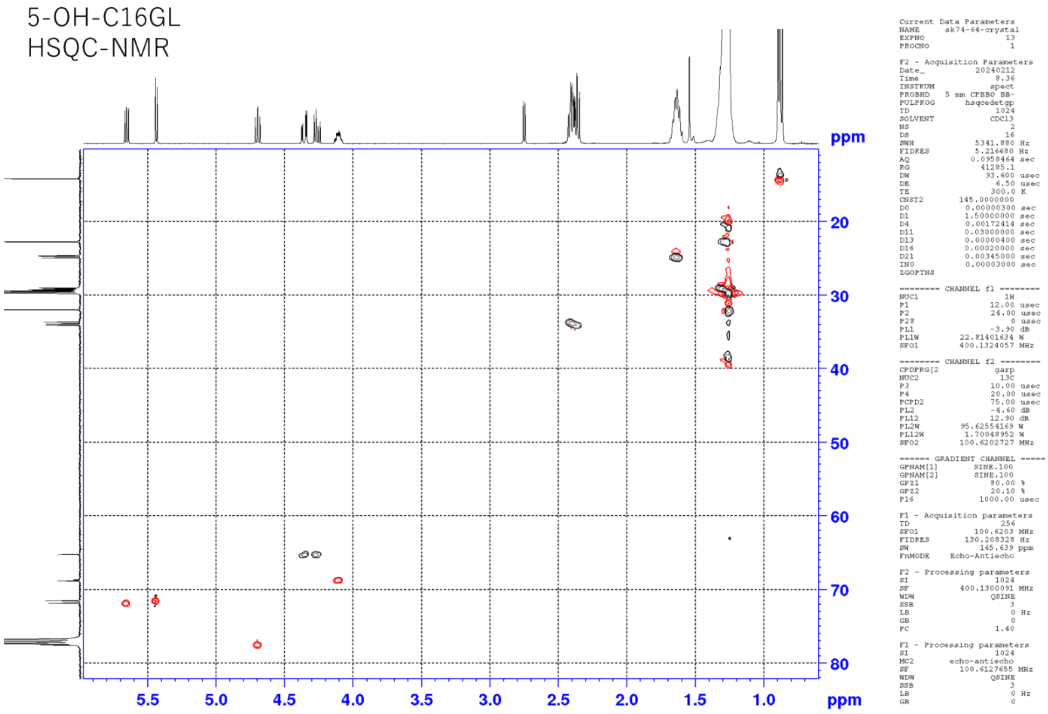

Figure S34. HSQC-NMR chart of 5-OH-C16GL (**7**).

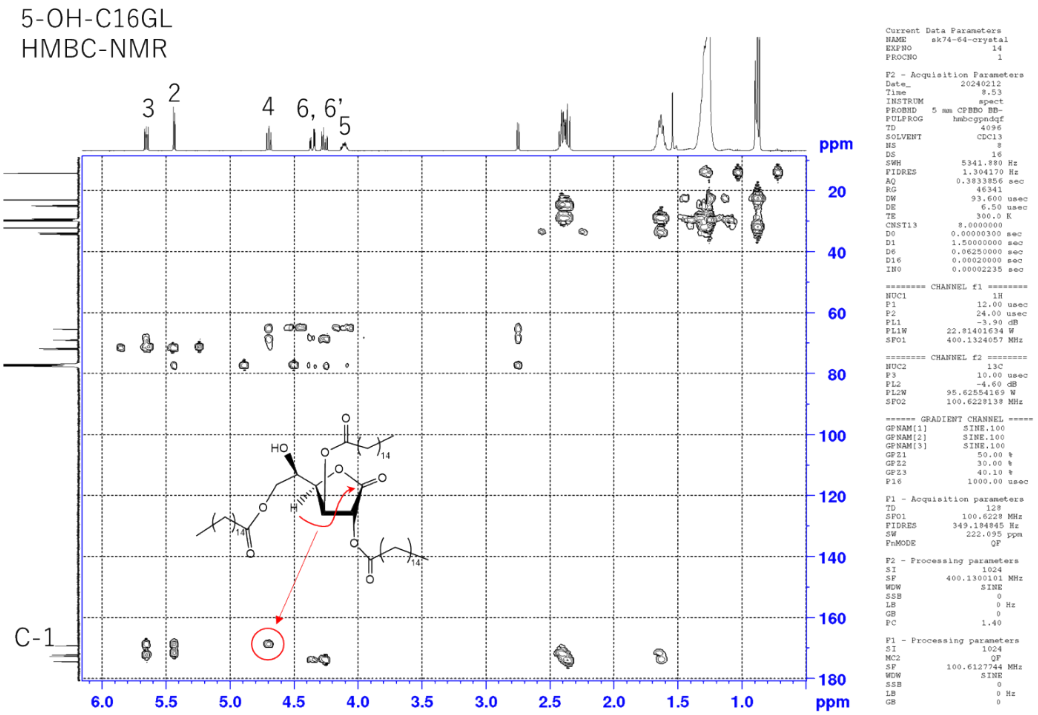

Figure S35. HMBC-NMR chart of 5-OH-C16GL (**7**).

2. Additional figures

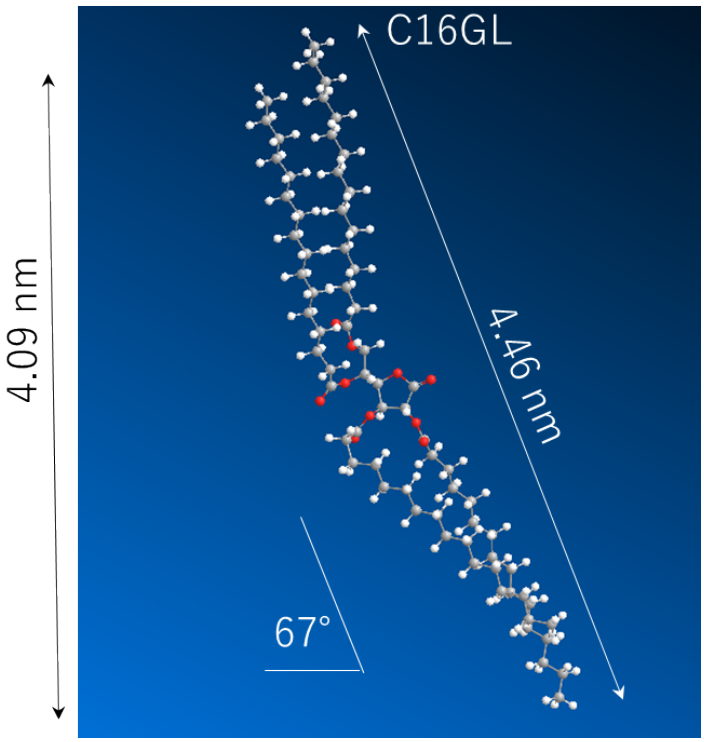

Figure S36. The ideal structure of C16GL (**4**) with the lowest thermal energy, calculated using MOPAC in Chem3D software (PerkinElmer Software).

Mopac Interface: Heat of Formation = −735.16404 Kcal/Mol.

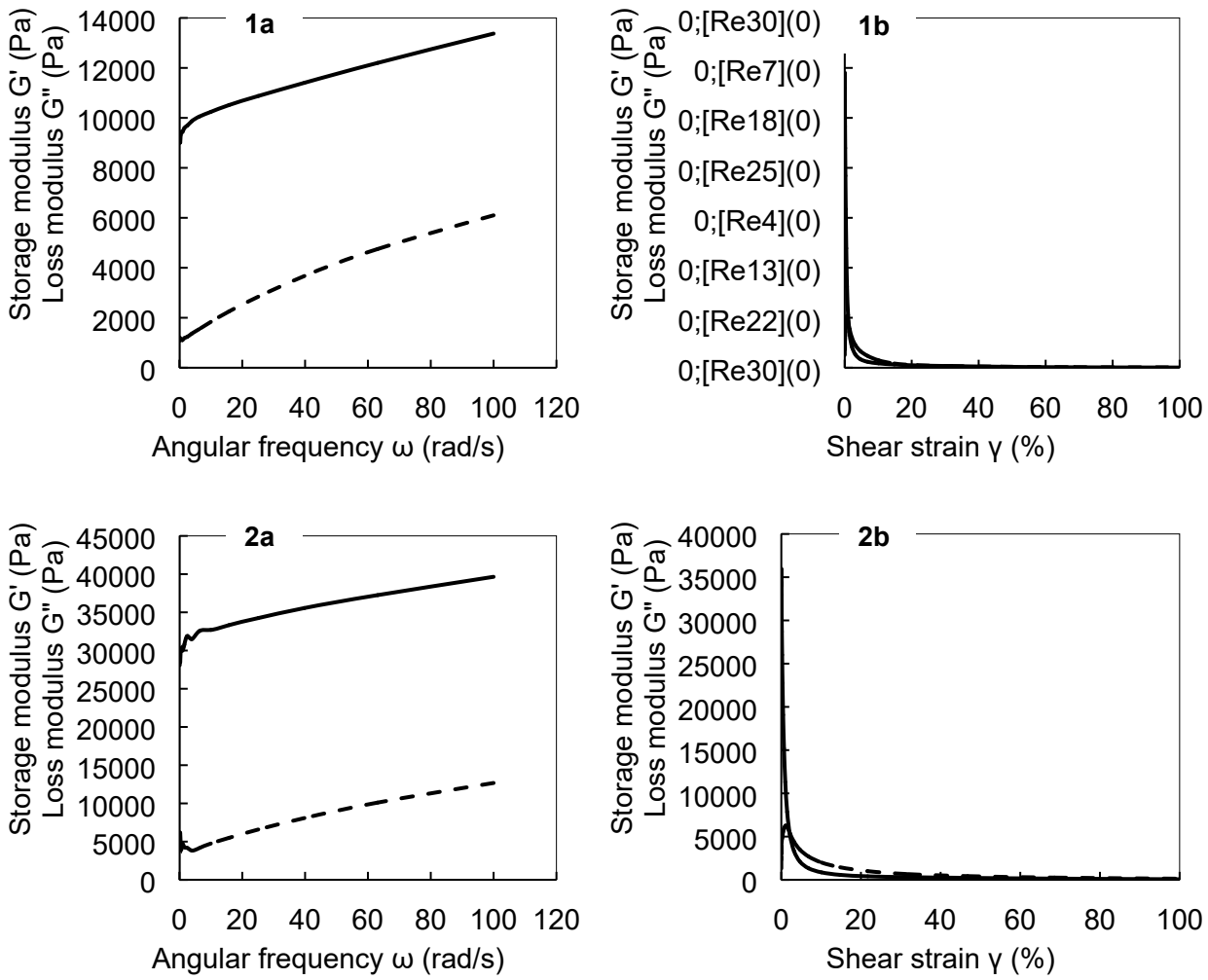

Figure S37. Rheological measurements using a rheometer. Left column (**1a** and **2a)**: Angular frequency (ω) dependent storage modulus G′ (solid line) and loss modulus G″ (dashed line). Shear strain (γ) = 0.1%, gap = 0.76 mm, temperature = 20°C, 50 mm diameter parallel plate. **1a**: 5 wt% C16GL (**4**) in liquid paraffin #350 gel. **2a**: 5 wt% C18GL (**5**) in liquid paraffin #350 gel. Right column (**1b** and **2b)**: Shear strain (γ) dependent storage modulus G′ (solid line) and loss modulus G″ (dashed line). Angular frequency (ω) = 0.5 rad/s, gap = 0.76 mm, temperature = 20°C, 50 mm diameter parallel plate. **1b**: 5 wt% C16GL (**4**) in liquid paraffin #350 gel. **2b**: 5 wt% C18GL (**5**) in liquid paraffin #350 gel.

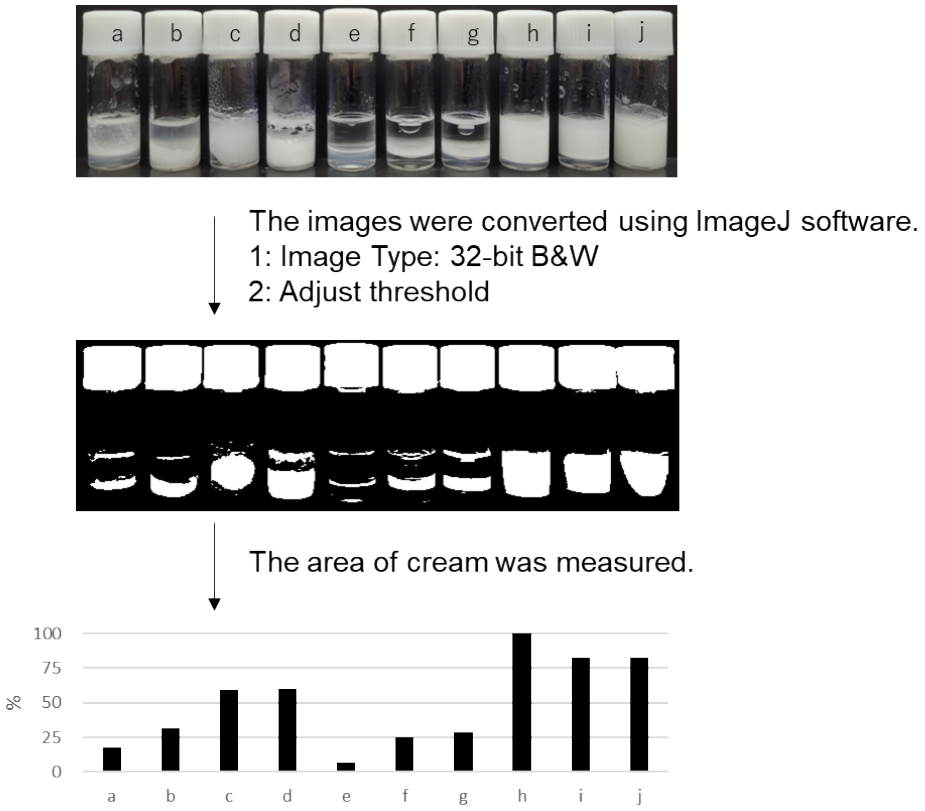

Figure S38. How to determine the area of the cream. After the image was converted using ImageJ software, the area of the cream was measured and graphed.

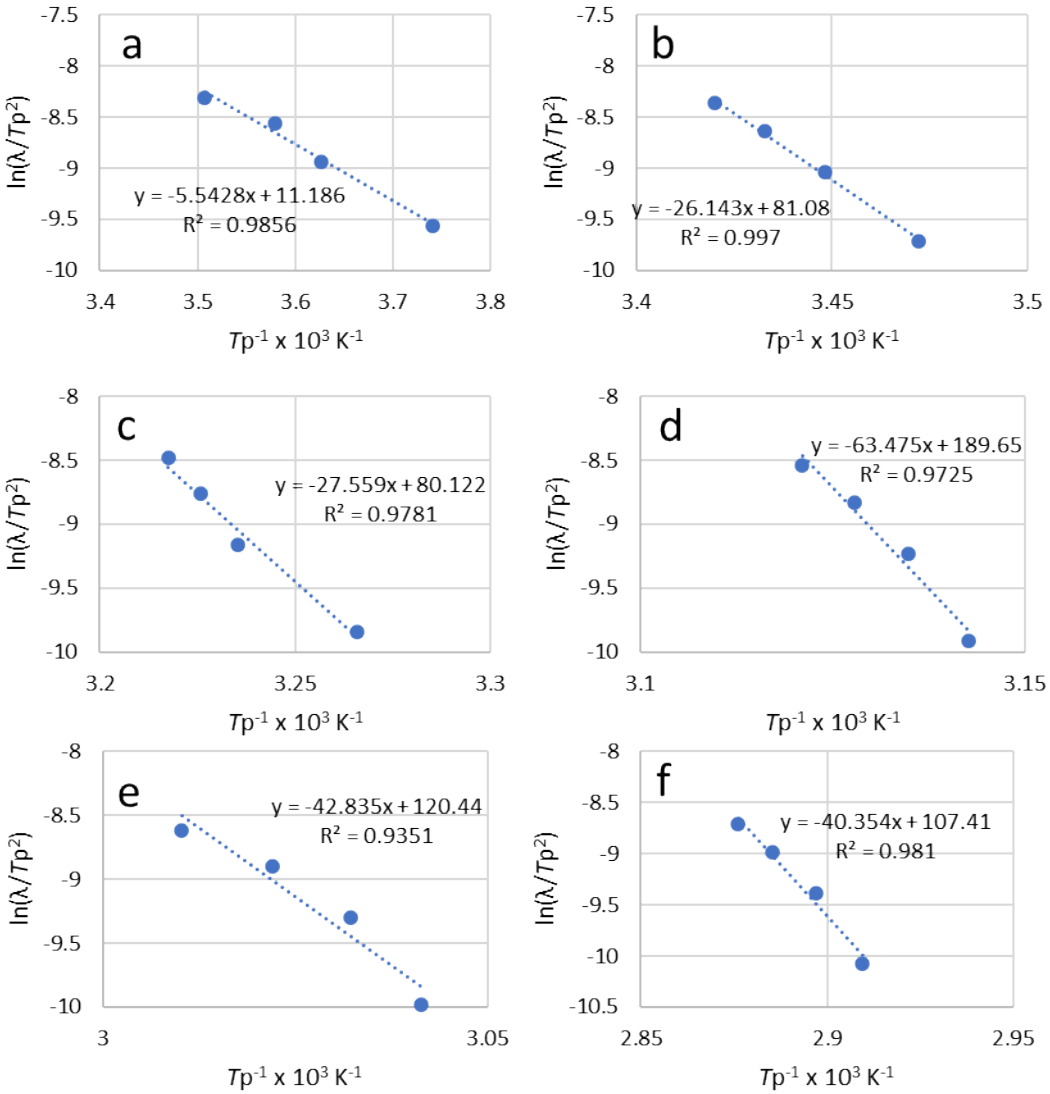

Figure S39. Kissinger plots to determine the activation energy of cold crystallization in DSC at different heating rates. The activation energy is obtained by multiplying the slope by the gas constant, R = 8.314 J K^{-1} mol^{-1}. T_p = peak cold crystallization temperature on heating [K], λ = temperature rate during heating [K min^{-1}]. a: C10GL (**1**), b: C12GL (**2**), c: C14GL (**3**), d: C16GL (**4**), e: C18GL (**5**), f: C22GL (**6**).

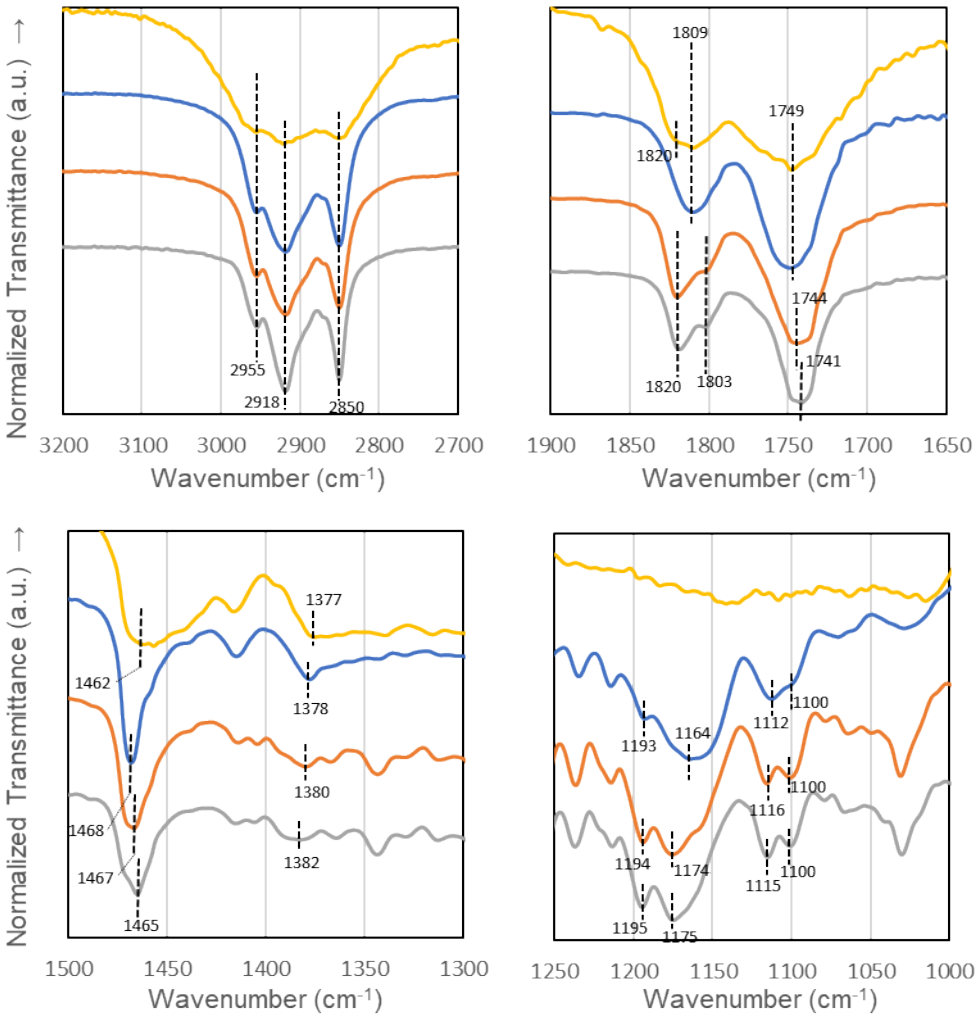

Figure S40. FT-IR spectra of type I, type II, and type III crystals and solution (at 100°C) of C18GL (**5**). Type I crystal (blue line). Type II crystal (orange line). Type III crystal (gray line). Solution at 100°C (yellow line).